MULTIPLE FLOW EQUILIBRIA IN THE TROPICAL CIRCULATION AND MONSOON

Zhu Baozhen (朱抱真)

Institute of Atmospheric Physics, Academia Sinica, Beijing

Zhao Jingxia (赵景霞)

Beijing Institute of Meteorology, Beijing

Received August 1, 1985

ABSTRACT

The aim of this paper is to examine whether an axisymmetric tropical model with thermal driving and orographic forcing can produce multiple equilibria in relation to the monsoon circulation over South Asia. The model is an equivalent barotropic balanced equatorial β-plane model. It shows that there may exist multiple flow equilibria for a given driving, of which two may be stable: one corresponds to the summer monsoon, and the other to the winter monsoon circulation. The transition between them is also discussed.

I. INTRODUCTION

Multiple equilibria of a forced, dissipative atmospheric system studied by Charney and others (1979-81) provided us a new insight into the dynamics of the atmospheric circulation. They developed a theory to explain the mid-latitude blocking and index cycle, and showed that, for certain range of forcings, there exist two stable and one unstable equilibrium states.

It is of great interest to study whether there are multiple stationary equilibria in the tropical circulation, and if so, what their nature is in relation to monsoon. Goswami (1983) examined the possible existence of the multiple equilibria in a two-layer axisymmetric model on an equatorial β-plane. The model did not take any mountains and land-sea thermal contrast into consideration. The effect of heating was mainly due to a Newtonian cooling with respect to a radiative equilibrium temperature, and to cumulus convection simply through the change of the value of static stability parameter. The model failed to show the existence of multiple equilibria in symmetric tropical circulations. Only one steady solution corresponding to the stable state was given by Goswami's study.

The aim of this paper is to examine whether a symmetric tropical model with thermal and orographic forcings can produce multiple equilibria. Since the summer monsoon and winter monsoon currents in South Asia may be considered as two different equilibrium states, we want to know whether the multiple equilibrium theory can explain monsoonal circulation over South Asia.

II. THE EQUATORIAL BALANCED MODEL

Using a barotropic semi-geostrophic symmetric model, we have the following basic equa-

tions:

$$\frac{\partial u}{\partial t}+v\frac{\partial u}{\partial y}-\beta yv=-ru,$$

$$\beta yu=-\frac{\partial \phi}{\partial y}, \tag{1}$$

$$C_0^2\frac{\partial v}{\partial y}-v\frac{\partial \phi_s}{\partial y}=-\varepsilon\phi-Q.$$

The third equation in (1) is derived from the continuity equation considering the forcing effect of orography and heating (Kasahara, 1966; Gill, 1980; Philander, 1984). However, we neglect the small term $v\,\partial\phi/\partial y$, the symbol $\phi_s=gh$, in which h is the mountain height. The coefficient for Rayleigh friction is r and the coefficient for Newtonian cooling is ε. Q is the prescribed thermal forcing, which may be considered as a heat source (sink) in the lower troposphere when $Q>0$ ($Q<0$). $C_0=\sqrt{gH}$ is the long gravity wave speed, where H is the equivalent depth of one-layer atmosphere. Matsuno (1966) showed that the equations governing the tropical motion may be decomposed into a series of vertical modes. The horizontal structure of each mode is described by the shallow-water equations with different equivalent depth of the vertical mode as its scale height. Therefore we may choose the suitable value of H to simulate the lower tropospheric motions.

From the equation system (1) we can derive an equatorial balanced model as follows:

$$\frac{\partial^2 u}{\partial t\partial y}+v\frac{\partial^2 u}{\partial y^2}+\frac{\partial v}{\partial y}\frac{\partial u}{\partial y}-\beta y\frac{\partial v}{\partial x}-\beta v=-r\frac{\partial u}{\partial y},$$

$$\frac{\partial^2 \phi}{\partial y^2}+\beta y\frac{\partial u}{\partial y}+\beta u=0, \tag{2}$$

$$C_0^2\frac{\partial v}{\partial y}-v\frac{\partial \phi_s}{\partial y}=-Q-\varepsilon\phi.$$

We expand the variables u, v, ϕ, ϕ_s, and Q by using orthogonal functions. In this paper, solutions will be found for the particularly simple case that only involves parabolic cylinder function up to order two, and thus we have a set of low order orthogonal functions:

$$\begin{pmatrix} u \\ \phi \end{pmatrix}=\sum_{i=1,2}\begin{pmatrix} u_i \\ \phi_i \end{pmatrix}D_i,$$

$$v=\sum_{i=0,1}v_iD_i,$$

$$\phi_s=\sum_{i=1,2}\phi_{si}D_i, \tag{3}$$

$$Q=\sum_{i=0,1}Q_iD_i,$$

where D_i is parabolic cylinder functions. The functions up to order two are given by

$$D_0,D_1,D_2=(1,y,y^2-1)\exp\left(-\frac{1}{4}y^2\right).$$

The highly truncated system (3) chosen above is the simplest one for the tropical monsoon over southern Asia to retain the following important characteristics:

(1) $u_{1,2}$ and $v_{0,1}$ may indicate general structures of lower tropospheric current, especially with a cross equatorial current by the component v_1;

(2) Q_0 may indicate the meridional insolation over the equatorial belt; and Q_1 may be the thermal effect of the land-sea contrast over the two hemispheres, a heat source (sink) over the Northern (Southern) Hemisphere;

(3) The combination of ϕ_{B1} and ϕ_{B2} roughly indicates a mountain ridge to the north of the equatorial belt and a valley to the south.

We apply a scaling procedure:

$$y=L\tilde{y},\quad (u,v)=u(\tilde{u},\tilde{v}),\quad t=\frac{L}{u}\tilde{t},\quad \phi=u^2\tilde{\phi},$$

and then we have the nondimensional equation for (3)

$$\begin{aligned}
&\frac{\partial^2\tilde{u}}{\partial\tilde{t}\partial\tilde{y}}+\tilde{v}\frac{\partial^2\tilde{u}}{\partial\tilde{y}^2}+\frac{\partial\tilde{v}}{\partial\tilde{y}}\frac{\partial\tilde{u}}{\partial\tilde{y}}-\tilde{\beta}\tilde{v}-\tilde{\beta}\tilde{y}\frac{\partial\tilde{v}}{\partial\tilde{y}}=-\tilde{r}\tilde{u},\\
&\tilde{\beta}\tilde{u}+\tilde{\beta}\tilde{y}\frac{\partial\tilde{u}}{\partial\tilde{y}}=-\frac{\partial^2\tilde{\phi}}{\partial\tilde{y}^2},\\
&\frac{\partial\tilde{v}}{\partial\tilde{y}}+\tilde{v}\frac{\partial\tilde{\phi}_B}{\partial\tilde{y}}=-\tilde{Q}-\tilde{\varepsilon}\tilde{\phi},
\end{aligned}\tag{4}$$

where

$$\tilde{\beta}=\frac{\beta L^2}{U},\quad \tilde{r}=r\frac{L}{U},\quad \tilde{\varepsilon}=\frac{\varepsilon UL}{C_0^2},\quad \tilde{\phi}_B=\frac{\phi_B}{C_0^2}=\frac{h}{H},\quad \tilde{Q}=\frac{QL}{C_0^2U}.$$

For convenience, we drop all the symbols "~" below. By substituting (3) into (4), and integrating them, we obtain the low-order model equations as follows:

$$\begin{aligned}
&\frac{\partial u_1}{\partial t}=-\frac{35}{9\sqrt{6}}v_0u_2-\frac{8}{9\sqrt{6}}v_1u_1+\beta v_0-ru_1,\\
&\frac{\partial u_2}{\partial t}=\frac{4}{3\sqrt{6}}v_0u_1+\frac{8}{9\sqrt{6}}v_1u_2+\frac{1}{2}\beta v_1-ru_1,\\
&\beta u_1=\frac{3}{2}\phi_1,\\
&\beta u_2=\frac{5}{2}\phi_2,\\
&v_0=2\varepsilon\phi_1+2Q_1-\frac{4}{\sqrt{6}}v_0\phi_{B2},\\
&v_1=-2Q_0+\frac{4}{3\sqrt{6}}v_0\phi_{B1}+\frac{4}{\sqrt{6}}v_1\phi_{B2}.
\end{aligned}\tag{5}$$

The above system contains two prognostic and four balanced equations. Further studies are made in this paper by using (5).

III. MULTIPLE EQUILIBRIA OF BALANCED MODEL

Rewriting equations (5), we have

$$\begin{aligned}
\frac{\partial u_1}{\partial t} &= A_0 + A_1 u_1 + A_2 u_2 + A_{12} u_1 u_2 + A_{11} u_1^2, \\
\frac{\partial u_2}{\partial t} &= B_0 + B_1 u_1 + B_2 u_2 + B_{12} u_1 u_2 + B_{11} u_1^2, \\
\phi_1 &= \frac{2}{3}\beta u_1, \\
\phi_2 &= \frac{2}{5}\beta u_2, \\
v_0 &= f_1 u_1 + G_1, \\
v_1 &= f_2 u_2 + G_2.
\end{aligned} \tag{6}$$

where

$$f_1 = \frac{4}{3}\varepsilon\beta \Big/ \left(1 + \frac{4}{\sqrt{6}}\phi_{B2}\right), \qquad f_2 = \frac{8}{3\sqrt{6}} f_1 \phi_{B1} \Big/ \left(1 - \frac{4}{\sqrt{6}}\phi_{B2}\right),$$

$$G_1 = -2Q_1 \Big/ \left(1 + \frac{4}{\sqrt{6}}\phi_{B2}\right), \qquad G_2 = \left(-2Q_0 + \frac{8}{3\sqrt{6}} G_1 \phi_{B1}\right) \Big/ \left(1 - \frac{4}{\sqrt{6}}\phi_{B2}\right),$$

$$A_0 = \beta G_1, \qquad B_0 = \frac{1}{2}\beta G_2,$$

$$A_1 = \beta f_1 - \frac{8}{9\sqrt{6}} G_2 - r, \qquad B_1 = \frac{1}{2}\beta f_2 + \frac{4}{3\sqrt{6}} G_1,$$

$$A_2 = -\frac{35}{9\sqrt{6}} G_1, \qquad B_2 = \frac{8}{9\sqrt{6}} G_2 - r,$$

$$A_{11} = -\frac{8}{9\sqrt{6}} f_2, \qquad B_{11} = \frac{4}{3\sqrt{6}} f_1,$$

$$A_{12} = -\frac{35}{9\sqrt{6}} f_1, \qquad B_{12} = \frac{8}{9\sqrt{6}} f_2.$$

In equilibrium, we could have a cubic equation for u_1 resulting from the above equations:

$$a_0 u_1^3 + a_1 u_1^2 + a_2 u_1 + a_3 = 0 \tag{7}$$

where

$$a_0 = B_{12}A_{11} - B_{11}A_{12}, \qquad a_1 = B_{12}A_1 + B_2 A_{11} - B_{11}A_2 - B_1 A_{12},$$
$$a_2 = B_{12}A_0 + B_2 A_1 - B_0 A_{12} - B_1 A_2, \qquad a_3 = B_2 A_0 - B_0 A_2.$$

The results are shown in Fig. 1. It can be seen that for an appreciable range values of Q (-0.25—-0.1), there are three separate equilibrium values of u_1.

The stability of the three steady states can be derived from the linearized equilibrium states in a small perturbation with

$$u_1 = \bar{u}_1 + u_1',$$

$$u_2=\bar{u}_2+u_2',$$

where $\bar{u}_1$ and $\bar{u}_2$ can be any of the equilibrium states.

The linearized system can be written as:

$$\frac{dG}{dt}=RG,$$

where

$$G=\begin{pmatrix}u_1'\\u_2'\end{pmatrix},$$

$$R=\begin{pmatrix}A_1+A_{12}\bar{u}_2+2A_{11}\bar{u}_1 & A_2+A_{12}\bar{u}_1\\ B_1+B_{12}\bar{u}_2-2B_{11}\bar{u}_1 & B_2+B_{12}\bar{u}_1\end{pmatrix}.$$

The eigenvalue of the matrix R determines the stability of the equilibrium state. It is a standard two-order dynamic system with the characteristic equations

$$\Delta=\begin{vmatrix}\lambda-(A_1+2A_{11}\bar{u}_1+A_{12}\bar{u}_2) & A_2+A_{12}\bar{u}_1\\ B_1+2B_{11}\bar{u}_1-B_{12}\bar{u}_2 & \lambda-(B_2+B_{12}\bar{u}_1)\end{vmatrix}=0,$$

and can be rewritten as

$$\lambda^2-T\lambda+D=0, \tag{8}$$

Table 1. The Equilibrium Solutions and Correspondent Eigenvalues Derived from Eq. (8)

Q_1	u_1	u_2	v_0	v_1	ϕ_1	ϕ_2	$(\lambda_r)_{max}$	λ_i
	−0.569	0.698	−1.085	0.076	−0.872	0.642	0.740	0.000
−0.20	0.084	1.416	0.420	0.159	0.128	1.303	−0.181	0.563
	−0.866	1.115	−0.349	0.038	−1.328	1.026	0.035	0.398
	−0.419	0.645	−0.075	0.081	−0.643	0.593	0.818	0.000
−0.15	0.135	1.391	0.374	0.151	0.207	1.279	−0.166	0.530
	0.850	1.184	−0.424	0.025	−1.303	1.090	−0.011	0.489
	−0.278	0.621	−0.049	0.085	−0.426	0.571	0.818	0.000
−0.10	0.190	1.357	0.330	0.145	0.291	1.249	−0.196	0.497
	0.838	1.232	−0.495	0.145	−1.270	1.134	−0.042	0.561
	−0.139	0.619	−0.025	0.089	−0.213	0.570	0.845	0.000
−0.05	0.246	1.314	0.287	0.138	0.377	1.209	−0.169	0.463
	−0.806	1.268	−0.563	0.004	−1.236	1.116	−0.065	0.626
	0.000	0.640	0.000	0.039	0.000	0.589	0.806	0.000
0.00	0.303	1.256	0.245	0.131	0.465	1.156	−0.083	0.423
	−0.784	1.295	−0.635	−0.007	−1.202	1.192	−0.083	0.689
	0.143	0.690	0.028	0.097	0.220	0.635	0.721	0.000
0.05	0.569	1.175	0.201	0.124	0.547	1.081	−0.032	0.366
	−0.764	1.317	−0.707	−0.189	−1.171	1.212	−0.098	0.751
	0.306	0.810	0.072	0.104	0.469	0.745	0.509	0.000
0.10	0.393	1.028	0.142	0.115	0.603	0.946	0.061	0.228
	−0.745	1.335	−0.780	−0.030	−1.143	1.228	−0.110	0.815

where

$$T \equiv A_1 + 2A_{11}\bar{u}_1 + A_{12}\bar{u}_2 + B_2 + B_{12}\bar{u}_1,$$
$$D \equiv (A_1 + 2A_{11}\bar{u}_1 + A_{12}\bar{u}_2)(B_2 + B_{12}\bar{u}_1) - (A_2 + A_{12}\bar{u}_1)(B_1 + 2B_{11}\bar{u}_1 + B_{12}\bar{u}_2).$$

When the maxi real part $(\lambda_r)_{max} < 0$, or $T < 0$ and $D > 0$, the equilibrium state is stable; otherwise it is unstable. Table 1 and Fig. 1 indicate the numerical results. We can find that the middle branch of Fig. 1 is unstable and the other two branches are stable. Thus we have succeeded in obtaining the multiple equilibria in the tropical balanced symmetric model.

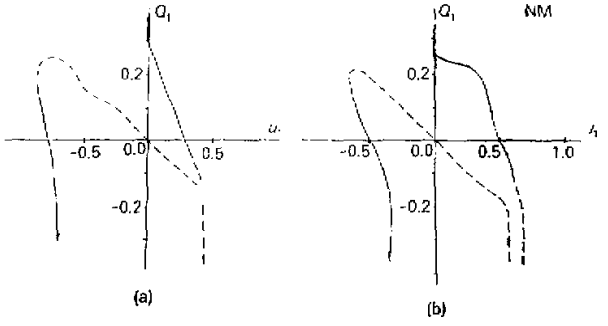

Fig. 1. The solution of multiple equilibria. $\varepsilon=0.3$, $r=0.2$, $Q_0=0.04$. Solid lines denote stable equilibrium. The dotted portions are unstable. (a) With mountains, $h_1=0.25$, $h_2=1/3h_1$; (b) Without mountains, $h_1=h_2=0$.

1. *Wind Structures of the Multiple Equilibria*

The structures of the lower level wind field are shown in Fig. 2. The left branch of the stable state seems to be the winter monsoon with the prevailing northwesterlies between 30°N and 15°N, the northeasterlies between 15°N and 6°S with a strong cross-equatorial current, and the intense westerlies to the south of 6°S.

The other stable state (right branch) appears to be the summer monsoon with the southeasterlies near the equatorial zone and the strong southwesterlies between 10°N and 30°N. The simulated convergence zone between the southeasterlies and the southwesterlies is located too far away from the equator, and the simulated cyclonic wind shear at 22°N latitude may be corresponding to the monsoon trough.

The model simulation of monsoonal current is seen to roughly agree with the observed South Asian monsoon, especially considering the simplicity of the model. The chief drawbacks are that the cross-equatorial NE and SE currents are too further southward and northward over the southern and northern sides of the equator.

The middle branch in Fig. 2 corresponds to the intermediate equilibrium, having a structure of weak easterlies over the Northern Hemisphere and weak westerlies over the Southern Hemisphere. This is an unstable steady state.

The above multiple equilibria have two stable equilibrium states corresponding to the winter and summer monsoonal circulations respectively, and one unstable state corresponding to a weak transitional circulation. From Fig. 1, we can see that the two stable equilibrium states occur only during the external heating Q_1 being small ($+0.15 - -0.05$). Outside this critical interval, there exists only one stable equilibrium state in which the summer or winter monsoon

determined by Q_1 is the heat or cold source. Therefore, we may conclude that during the transitional period, the heating contrast between the ocean and continent is very weak; there could have two equilibrium states under the same weak Q_1. Which state will be formed depends on the initial circulation type. A further discussion will be given in the following paragraph.

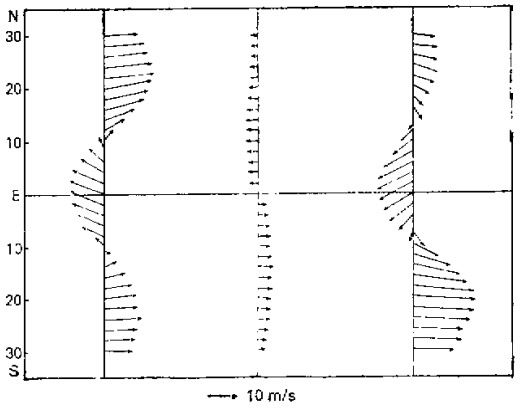

Fig. 2. Wind structures of the different equilibrium states.

2. *Thermal Forcing Instability*

It is important to examine the physical mechanism of the formation of the unstable equilibrium state. Since the "no mountain" case in Fig. 1b has also produced the unstable equilibrium states, we may conclude that the orographic instability is not a crucial one. For simplicity, we can assume $h=0$ in Eq. (8), and then we have

$$T=2r-\frac{4}{3}\varepsilon\beta(\beta-a_1\bar{u}_2),$$

$$D=\left(\frac{4}{3}\varepsilon\beta^2-b_1Q_0-\frac{4}{3}a_1\varepsilon\beta\bar{u}_2\right)Q_0-C_1\left(Q_1-\frac{2}{3}\varepsilon\beta\bar{u}_1\right)\left(Q_1-\frac{4}{3}\varepsilon\beta\bar{u}_1\right),$$

where a, b and c are different coefficient values. When $T>0$ and $D<0$, it will be unstable. The first condition is relatively simple—the steady state is unstable to the perturbation when $\bar{u}_2<\beta/a_1$, i.e. the zonal wind must be very weak; the second condition is considerably complex—it contains a relationship between the relative intensity of Q_1 and Q_0 and the steady currents $\bar{u}_1$ and $\bar{u}_2$. For further simplicity, we assume $\bar{u}_1=\bar{u}_2=0$, because they are fairly small in comparison with the first condition. Then it may be qualitatively known that the intensity of Q_1 must be smaller than a prescribed value.

We also calculated the barotropic instability conditions $\beta-\partial^2\bar{u}/\partial y^2=0$ from numerical results. Since $\beta-\partial^2\bar{u}/\partial y^2$ does not vanish anywhere in the middle branch of Fig. 2, we may suggest that the instability of the unstable equilibrium is not the simple barotropic instability of the zonal flow. The above analysis concludes that the instability seems to be a kind of land-sea thermal forcing instability under the weak zonal currents.

When the state is close to the unstable steady solution, it will make a transition to one of the other two stable equilibrium solutions. Which one of the two stable equilibrium solutions

the state will actually change into depends on the initial conditions of the state.

This idea may be confirmed further by numerically integrating Eq. (6) under the case with given initial states. Figure 3a shows two examples of such behavior for an experiment started from two different initial conditions with fixed external parameters. It is found that for $u_1(0) = 0.75$, say, an early winter situation, the $u_1(t)$ value approaches a steady equilibrium in the form of a slowly damped oscillation. The solution near $u_1(0) = -0.44$, say, an early summer situation, converges rapidly to the summer equilibrium.

Figure 3b shows the corresponding phase space (u_1, u_2) trajectories. The arrows indicate the direction of increasing time. Both of them spiral to the steady solutions, while there are more spirals in the early winter case, than in that of the early summer.

Thus we may infer that the transition of the buildup of summer monsoon seems to be more abrupt and steady than that of the winter monsoon.

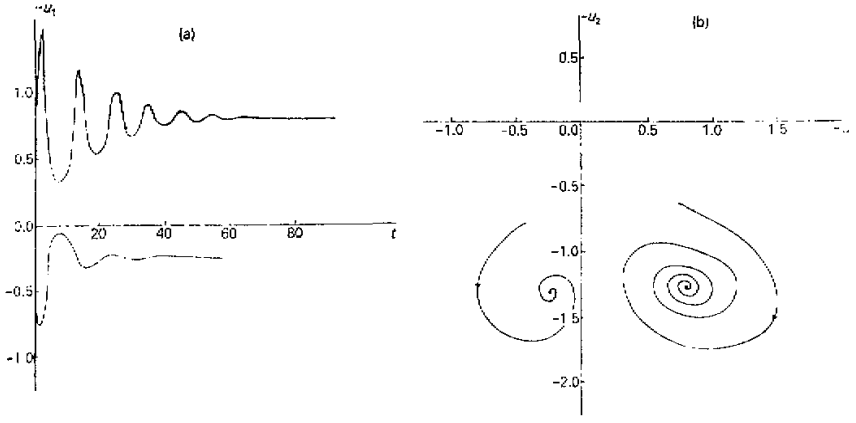

Fig. 3. Numerical integration starting from different initial conditions, a) transition of u_1 with time; b) space trajectories (as in Fig. 1, except for $Q_1 = -0.05$).

3. *Orographic Effects*

Considering the case without mountains, $h = 0$, the resulting stationary solutions are shown in Fig. 1b. Comparing it with Fig. 1a, we can see that orography would produce the nonsymmetric properties of the two stable equilibria:

(1) The intensity of u_1 in the summer monsoon is smaller than that in the winter monsoon when the mountain effects are considered.
(2) The summer monsoon sets up under the smaller land-sea heating contrast due to the mountain effects.

IV. NUMERICAL INTEGRATION FOR AN ANNUAL PERIODIC HEATING

A numerical experiment is also performed with the system or time-dependent equation (6) by introducing a prescribed annual periodic heating Q_1 to study the time-dependent solutions of the response to external forcings.

The prescribed annual periodic heating is expressed with

$$Q_1 = 0.25 \sin\left(\frac{2\pi t}{T}\right), \quad T = 365 \quad \text{days.}$$

It is combined with Q_0 to indicate roughly the seasonal variation of solar radiation and heating contrast between land and sea.

Figure 4 shows the annual variations of Q_1 and u_1. It is very interesting that:

(1) The irregular and nonsymmetric response of u_1 is linked with the regular and symmetric changes of Q_1;

(2) The sudden changes of the circulation during mid June and October just coincide with the well known observational aspects suggested by Yeh et al. (1959).

Let $h=0$; then we have the lowest curve in Fig. 4. Comparing it with the middle curve, it is worthy to note that the mountain effect is very important to the non-symmetric length of the winter and summer monsoons. Thus the orographic dynamic process is dominant during the sudden changes of atmospheric circulation in June and October over the South Asian region.

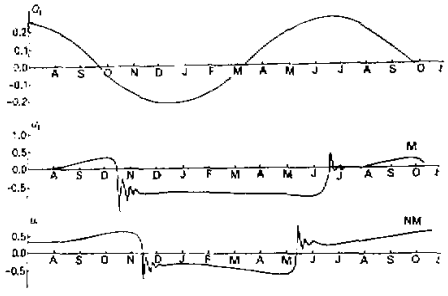

Fig. 4. Annual variations of Q_1 (upper) and related solutions of u component for the cases with mountains (middle) and without mountains (lower).

V. CONCLUSION

Non-linear properties of a simplified axisymmetric tropical model have been shown that a combination of thermal forcing and orography in a barotropic balanced model gives rise to multiple equilibrium states. One of these two equilibria can be associated with summer monsoon, while the other has a winter monsoon circulation. These two types of equlibrium can exist for a certain weak values of the thermal forcing parameters.

Owing to the two stable equilibria obtained, there must exist an intermediate unstable equilibrium, the instability is probably produced by the land-sea heating contrast under the stable equilibria. Once the atmosphere has come into one of these two stable equilibrium states, it is usually to remain there for a long period due to the stability of the flow, corresponding to the persistence of monsoon.

The effect of mountains modifies the structure and the evolution of the thermal monsoon. Orographical condition produces the nonsymmetric properties of the seasonal variations and the sudden buildup of the monsoon circulation in June and October over South-Asia.

The authors wish to thank Profs. D.R. Johnson and J.A. Young of the Department of Meteorology, University of Wisconsin, as well as to Profs. Y. Yanai, and A. Arakawa of the Department of Atmospheric Science, UCLA for their valuable discussions when the first author visited the two universities in 1985. Thanks are also to Mr. Shen Rujin for his beneficial suggestions.

REFERENCES

Charney, J.G. and Devore G. (1979), Multiple Flow Equilibria in the Atmosphere and Blocking, *JAS*, **36**: 1205–1216.

Charney, J.G. and Straus D.M. (1980), Form–Drag Instability, Multiple Equilibria and Propagating Planetary Waves in Baroclinic, Orographically Forced, Planetary Wave Systems, *JAS*, **37**: 1157–1176.

Gill, A.E., (1980), Some Simple Solutions for Heat-Induced Tropical Circulation, *QJRMS*, **32**:447–462.

Goswami, B.N., (1983), Theoretical Study of Multiple Equilibria in Simple Axisymmetric Tropical Circulations, *Tellus*, 35:119–135.

Kasahara, A., (1966) The Dynamical Influence of Orography on the Large Scale Motion of the Atmosphere, *JAS*, **23**:259–271.

Matsuno, T. (1966), Quasi-geostrophic Motion in Equatoial Areas, *JMSJ*, **44**:25–43.

Philander, S.G.H. et al., (1984), Unstable Air–Sea Interaction in the Tropics. *JAS*, **41**:604–613.

Yeh T.C., Tao S.Y and Li M.T. (1959), The Abrupt Change of Circulation over the Northern Hemisphere during June and October. In: *The Atmosphere and the Sea in Motion*, Vol. (B, Bolin, Ed.) New York, Rockefeller Inst. Press. 249–267.